

# Using Numerical Inverse Laplace for Optimizing the Current Control in Grid Coupled Inverters

Jean Marie Vianney Bikorimana  
Ghent University  
Ghent, Belgium  
and University of Rwanda, Rwanda

Alex Van den Bossche  
Ghent University  
Ghent, Belgium

**Abstract**— A number of control circuits can be well analyzed in a Fourier transfer function, but they have problems in being analyzed in an analytical inverse Laplace response as they contain distributed poles and zeroes, coming from a time delay or other effects. An example is the control of converters with filter circuits. In this paper, a control is shown in a PV converter with a very small DC link capacitor which is normally difficult to stabilize due to the presence of resonance effects of filters. It is observed that a second order high pass filter feedback stabilizes well parasitic resonances, even if their frequency is not very low compared to the switching frequency. A numeric inverse Laplace can be implemented in almost any mathematical program. This paper shows how parameters can be obtained from a step response using the numerical inverse Laplace and be used in Matlab simulation. It shows the complementarity between two methods.

**Keywords**—Numerical Inverse Laplace Transform; Step response; PV converters.

## I. INTRODUCTION

Different methods exist to analyze the stability or step responses in converters [5],[8] and [9]. It may be by classical methods or by simulation. Classical methods are limited if distributed poles and zeroes are present [10], in the case of delays, fractional differentials, and complex transmission line effects, such as a skin-effect [3],[4]. In the case of simulations, the researchers have to be able to distinguish between a non-convergence of solvers, instability and inaccurate solutions [7]. For this reason, they are interested in analyzing a topology using an independent method, which may be a higher accuracy and possibly also be faster. This paper demonstrates the complementarity between two methods used to test the step feedback responses of a PV boost Converter found in [1]. The paper focuses on a topology used for a Reduced Losses technique in PV Converters by Modulation of the DC Link Voltage [1]. The topology has two main parts, a boost and an inverter. The aim is to control the current in inductor L2 while switching Q1, so that the DC link voltage follows the grid voltage during the top of the period and the bridge does not have to switch. Normally, it is expected that it is not easy to directly control the current in L2 since the system is third order dynamic type. The paper analyses the current control feedback behavior of the boost converter. To create enough phase margin, a second high pass filter type has been introduced in the topology [Fig.2]. The proposed controller uses a small film capacitor C2= 20  $\mu$ F and the storage is done at level of C1= 2200  $\mu$ F, L1=600  $\mu$ H and L2= 1400  $\mu$ H. One test was carried out using Matlab/Simulink<sup>TM</sup>.

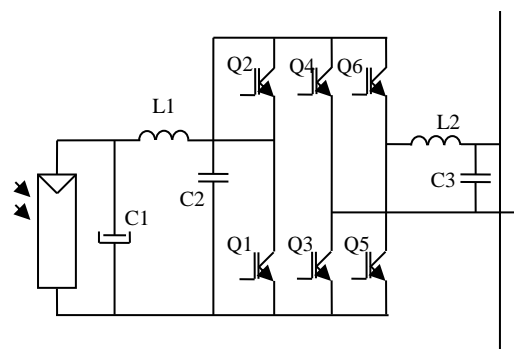


Fig.1 Single phase PV converter using a three-phase bridge [1]

Some solvers in Matlab/Simulink<sup>TM</sup> are appropriate to some types of problems: stiff or non-stiff systems. In this case the solver ODE 23s gave the best results. The reason is that power electronic circuits may be of a non-linear and discontinuous nature. On the other hand, the user can be challenged and losing time by choosing the right solver. Finding the right parameters may not be easy without a view on the phase and amplitude margin, it is even not guaranteed that a stable solution can be found. For small signals, the power electronic converters behave often in a linear way. This means that those cases can also be analyzed using transfer functions as reference cases to test the simulations. As calculating transfer functions and inverse Laplace goes fast, it is possible to use it to search for the approximate values for feedback topologies and parameters. The inverse Laplace Transform was known for centuries and it has many algorithms which are often complex [2],[12]. Nevertheless, the used inverse Laplace Transform, in this paper, is based on a simple definition. It shows how any scientist or engineer can implement the numerical inverse Laplace Transform as a simple and fast tool to test a step response or other responses of an electrical, electronic or mechanical circuit more than what some complex tools do. Matlab Simulink<sup>TM</sup> has been mentioned earlier as another tool that can be used. Numerical Inverse Laplace Transform

The numerical Inverse Laplace Transform has many possible algorithms. The most popular are: Talbot, Week and Post's methods [2]. However, all of them are based on the Laplace Transform definition. Eq.1 gives the definition of the unilateral Laplace which is mostly used [2]. Bidirectional

Laplace transform is equivalent to the unidirectional type if the poles and zeros are symmetrical.

$$\mathcal{L}[f(t)] = F(p) = \int_0^{\infty} f(t) e^{-pt} dt \quad (1)$$

Where f(t) is a function with a real argument, t.

F(p) is a function with a complex argument,  $p = \sigma + i2\pi v$  with  $(\sigma, v) \in \mathbb{R}^2$ . Using a Fourier transform operator, Eq.1 can be written as follows:

$$\mathcal{L}[f(t)] = F(\sigma + i2\pi v) = \int_0^{\infty} f(t) e^{-2i\pi vt} dt \quad (2)$$

Eq.2 is a link between Fourier and Laplace Transforms. After some mathematical deduction [2], the inverse Laplace transform is expressed by the following equation:

$$\begin{aligned} \mathcal{L}^{-1}[F(p)] &= f(t) = \int_0^{\infty} F(\sigma + i2\pi v) e^{(\sigma + i2\pi v)t} dv \\ &= \frac{1}{2i\pi} \int_{-\sigma}^{-\sigma + j\infty} F(p) e^{pt} dp \end{aligned} \quad (3)$$

Programs such as Mathcad14 do not support equations with complex limits, but it can be converted to real limits in (4). For a frequency range between  $\omega_{min}$  and  $\omega_{max}$  which may be 0.01 rad/s to 100 Mrad/s should be sufficiently wider than the applied signal type. Then the following equation can be obtained:

$$f(t) = \frac{2}{2\pi} \int_{\omega_{min}}^{\omega_{max}} \left[ \frac{e^{(\sigma + i\omega)t}}{(\sigma + i\omega)} \cdot (F(\sigma + i\omega)) \right] d\omega \quad (4)$$

Where  $\omega = 2\pi v$ , but the limits are converted to real values to have some meanings. The integral can also be replaced by a sum, with a frequency which is distributed in a logarithmic way:

$$\begin{aligned} f(t) &= \frac{2}{2\pi i} \sum_{m=0}^n \left[ (P(m + 0.5) - \right. \\ &\left. P(m - 0.5)) \cdot \frac{e^{P(m)t}}{P(m)} \cdot (f(P(m))) \right] \end{aligned} \quad (5)$$

Where: m and n are real numbers

$$P(m) = \sigma + i \cdot 10^{m \log\left(\frac{\omega_{max}}{\omega_{min}}\right)} \quad (6)$$

Considering the previous frequency range the Eq.6 can be written as follows:

$$P(m) = \sigma + i \cdot 10^{\frac{m}{400} - 2} \quad (7)$$

## II. CURRENT CONTROL WITH A SECOND HIGH PASS FILTER FEEDBACK TRANSFER FUNCTION OF THE BOOST CONVERTER

Fig.2 and Fig.3 show the boost converter with a second high pass filter feedback used to deduct its transfer function. It is not obvious that the current in L2 is intended be controlled by switching the current in L1.

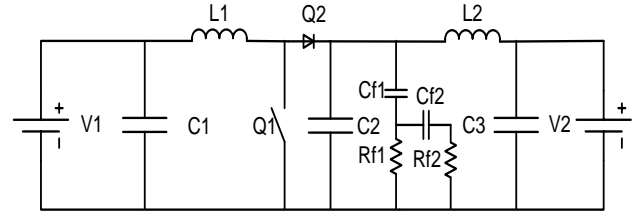


Fig.2 Buck Boost converter of the Topology

For small signal deviations and continuous conduction mode [CCM], the scheme can be converted into Fig.3:

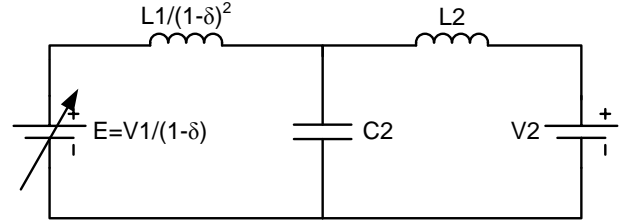


Fig.3 Equivalent Circuit of Buck Boost Converter of the Topology

To stabilize the LC filter and to compensate its calculation delay, the high pass filter transfer equation is expressed in Eq.8. The single order high pass filters did not give enough phase advance.

$$H_{hp}(s) = \frac{1}{1 + \frac{1}{\lambda_1 p}} \cdot \frac{1}{1 + \frac{1}{\lambda_2 p}} \cdot e^{-Td_1} \quad (8)$$

Where, Td1 is a delay for digital sampling,  $\lambda_1 = 5 \cdot 10^{-5}$  and  $\lambda_2 = 1 \cdot 10^{-4}$  are time constant for the high pass filter 1 and 2 respectively [1].

The values of the second hang pass filter are: Rf1=5E3 Ohms; Rf2=50E3 Ohms; Cf1=10E-9 F, Cf2= 1E-9 F.

Considering Fig.3, the dynamic behavior of the topology and its CCM case, the transfer function can approximately be formulated as follows:

$$\begin{aligned} H(p, \delta) &= \frac{RL2 + pL2}{\frac{(RL1 + pL1) \cdot [p \cdot C2 \cdot (RL2 + s \cdot L2)]}{(1 - \delta)^2} + RL2 + pL2} \end{aligned} \quad (9)$$

Where R, L1, L2,  $\delta$  are parameters of the topologies.

Eq.10 is a product of Eq.8 and Eq.9 which expresses the open loop system transfer function.

$$TF = H_{(hp)} * H(p, \delta) \quad (10)$$

The bode diagrams of the open loops of the high pass filter in Fig.4 and Fig.5 can help to figure out the current feedback loop transfer function.

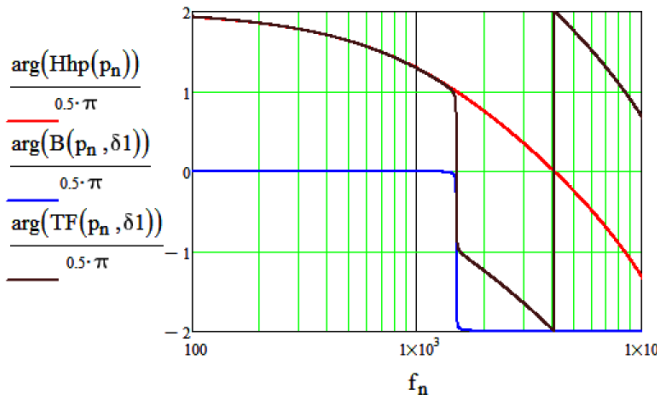


Fig.4 TF1 open loop phase Vs frequency

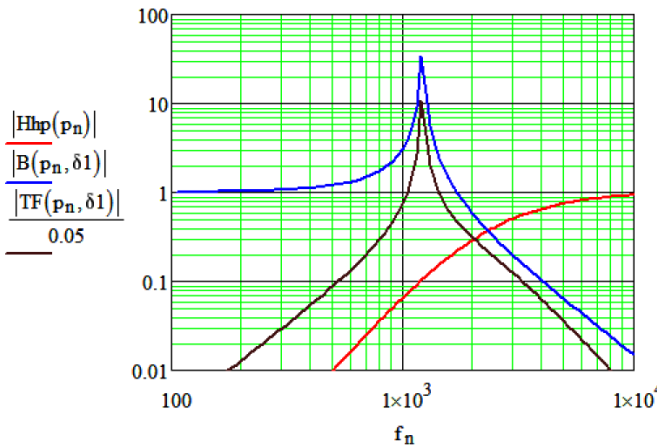


Fig.5 TF2 open loop magnitude Vs frequency

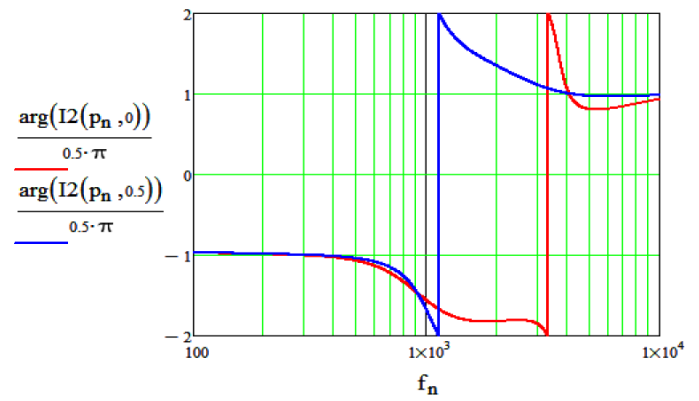


Fig. 6 I2(p,delta) closed loop phase Vs frequency

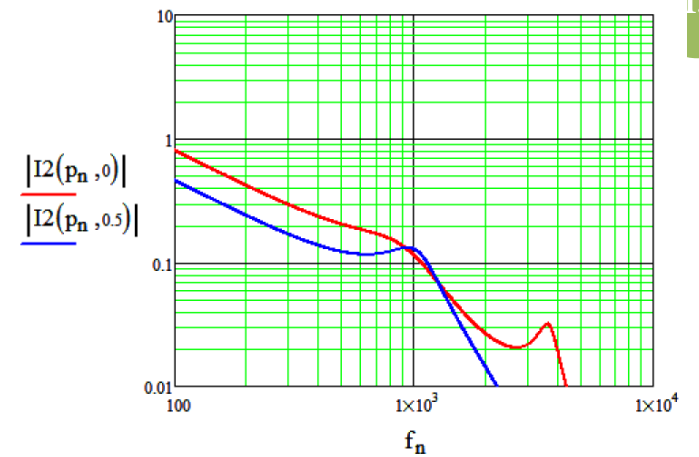


Fig.7 I2(p,delta) closed loop magnitude vs frequency

In fact, Fig. 4 and Fig. 5 give the stability limit information of the system. Around the gain margin of 12 the system oscillates. Therefore, the gain margin less than 12 can make the system stable. The chosen gain is 5 for the current feedback loop. The transfer function of the current feedback is found in Eq.11.

$$I2(p, \delta) = \frac{B(p, \delta)}{1 + B(p, \delta) * H_{hp}(p) * G_{hp}} * \frac{1}{RL2 + p * L2} \quad (11)$$

Where  $G_{hp}$  is the gain of the high pass filter.

The dynamic behavior in Fig.6 and Fig. 7 is found based on the Eq. 11. Since the feedback is a PI type, Fig. 6 and 7 present the limit of the resonant frequency which are useful to tune the PI parameters. Based on them, the PI transfer function is calculated [Eq.12]. PI together with the analog sampled second order high pass could be considered as PI on the current  $I_{l2}$  plus  $D^2$  at the level of voltage across C2. The D has been implemented in an analogue way to avoid delay while completing digital high pass filter actions. The programmer could sample the voltage across C2 and implement the high pass filter action, but anyhow an attenuation is needed. The direct sampling of the voltage and , a second order high pass filter would still result in an additional delay.

$$PI(p, \delta) = \left[ \frac{3000 \cdot (1 - \delta)}{P} + 4 \right] * e^{-pTd2} \quad (12)$$

Where  $Td2$  is the delay of the PI controller.

The Open Loop Transfer Function (OLG) of the current in the second inductor combined with the transfer function of the PI controller is in Eq.13.

$$OLG(p, \delta1) = I2(p, \delta) * PI(p, \delta) \quad (13)$$

For the tuned parameters, the system is stable. The pole is at one in left side. Fig.8 shows that for different values of delta, 0.0, 0.5, 0.8, the system is stable.

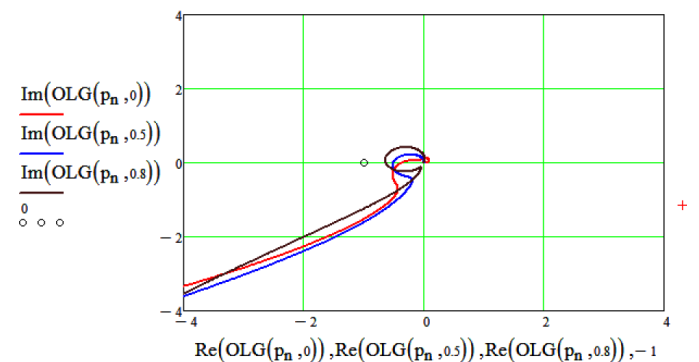


Fig.8 OLG Imaginary Vs Real part Nyquist

Then, the total feedback transfer function of the system becomes as follows:

$$TFI(p, \delta) = \frac{1}{1 + \frac{1}{OLG(p, \delta)}} \quad (14)$$

Eq.15 and 16 deduced when the Eq.4 and 5 are applied on Eq.14.

$$f(t, \delta) = \frac{2}{2\pi} \int_{\omega_{min}}^{\omega_{max}} \left[ \frac{e^{(\sigma+i\omega)t}}{(\sigma+i\omega)} \cdot (TFI(\sigma+i\omega, \delta)) \right] d\omega \quad (15)$$

$$f(t, \delta) = \frac{2}{2\pi i} \sum_{m=0}^n \left[ (P(m+0.5) - P(m-0.5)) \cdot \frac{e^{P(m)t}}{P(m)} \cdot (TFI(m, \delta)) \right] \quad (16)$$

The step response of the transfer function can be test with the following input signal, where a slow square wave is used instead of a step wave.

$$f(t) = \sum_{k=0}^{100} \frac{2}{2k+1} \cdot \sin[(2k+1) \cdot \omega \cdot t] \quad (17)$$

Where k is a real number,  $k \in \mathbb{R}$

The step response can as well be applied, but at least, 100 harmonics are needed at least to lower the Gibbs effects [11]. It is slow if a low frequency step wave is applied. It is, moreover, difficult to check if an overshoot is present or not. It can be formulated using a complex Fourier Transform [Eq.18]. Fig.9 results from Eq.18. It is obvious that the step response has periodically the Gibbs effects.

$$f(t) = \sum_{k=0}^{100} \frac{2}{2k+1} \cdot \text{Im}[TFI[(2k+1) \cdot i\omega \cdot t \cdot \delta] \cdot e^{(2k+1) \cdot i\omega \cdot t}] \quad (18)$$

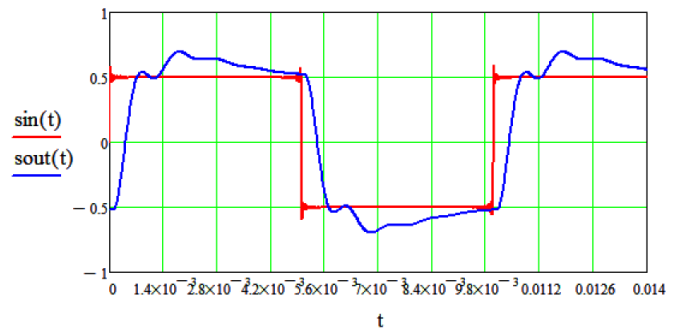


Fig.9 Step response at  $\delta = 0.5$

However, instead of using an sum of harmonics, also an inverse Laplace could be used. The inverse Laplace is going back from Laplace/frequency domain back to the time domain. Both Eq.15 and Eq.16 are used for the numerical Inverse Laplace transform. The first one is integral type with the limits, in this paper, are chosen to vary from  $10^{-2}$  to  $10^{-8}$  whereas for the second one, summation type, m varies from 0 to 4000. In fact, the interested frequencies are between 30 and 300 kHz. This means that 400 division /decades are more than sufficient. The equations gives the same results with a slight difference between the running time. One may be faster than the other depends on the boundaries applied on the integral as well as on the summation. Next section presents the results given by MatlabSimulink™.

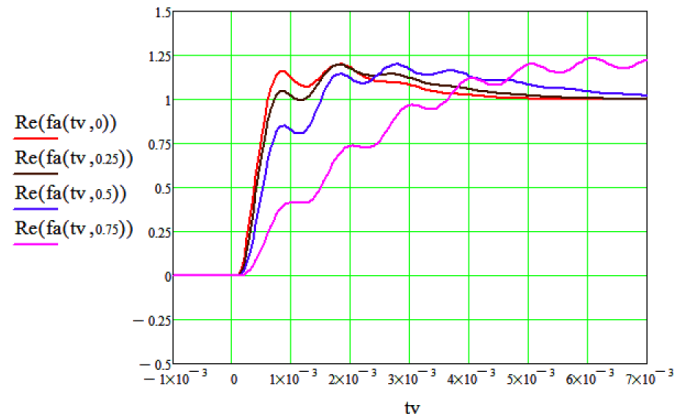


Fig.10 Step response of Eq.15 and Eq.16

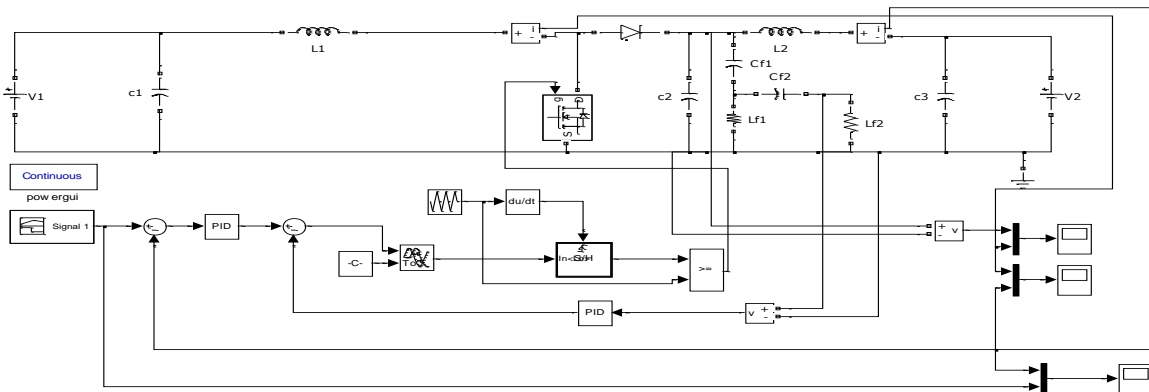


Fig.11 The PV converter current mode control block diagram in Matlab/Simulink™

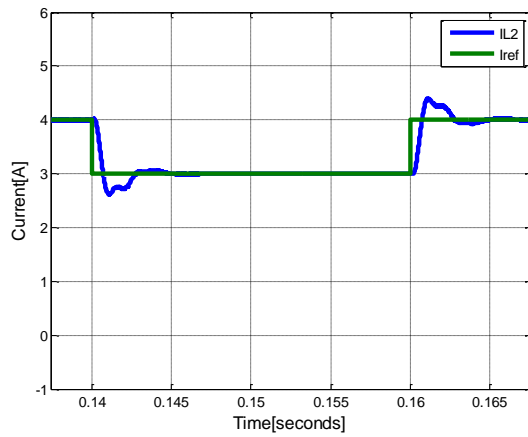


Fig.12 Iref and IL2 of the Boostconverter with  $\delta = 0.5$

The same test was firstly done in Matlab/Simulink™ to test the step response. Fig.11 shows the Matlab simulation block diagram of the boost converter. This method is mathematically easier than the previous method since for this method the transfer function deduction is not required. Nevertheless, choosing the right solver is a key task while Matlabsimulink™ is opted. Fig. 12 presents the simulation results. The parameters used for simulation are found in [1]. Different ODES have been used for this simulation. ODE 45 is designed for non-stiff problems [6]. Specific ODES of the implicit type have to be used for the stiff systems. The implicit solver grants the high stability for the oscillatory systems [7]. In this paper, the ODE 23S was used and it proved that the current control tuned parameters using numerical Laplace Transform make the system stable.

A special effect is that the numerical inverse Laplace always results in stable responses, even if the system is unstable, but it can be recognized as the system reacts before the step is applied, which is an a-causal effect. Also, other responses can be analyzed by adaptation of Eq.16. The step response was used to test the stability and the damping in a wide frequency range. In real PV converters, the set values will be rather sine waves, but one has to be sure that the system is well damped.

### III. CONCLUSIONS

There are different software and tools that engineers and scientists can use, the sequence of Nyquist, inverse numerical Laplace and Matlab Simulink is interesting. In a Nyquist plot the engineer can easily first tune the parameters to get the right phase and amplitude margin. After this, the step response can

be optimized by inverse Laplace using Mathcad or another type of software. Here, the numerical Inverse Laplace Transform is used with a simple definition. It was employed to tune parameters to stabilize a feedback in a PV converter system with filters, which is normally not easy to obtain. Afterwards, these parameters were used as an input for Matlab simulation including PWM. So, the stability of the system is in fact triple checked. The methods are complementary to each other proving that a current control with a second order high pass filter feedback of a boost converter is stable at different duty ratio values.

### ACKNOWLEDGMENT

The first author does acknowledge the BOF fund of Ghent University for funding the research.

### REFERENCES

- [1] Alex van den Bossche, Jean Marie Vianney B., Firgan Feradov, "Reduced losses in PV converters by modulation of the DC link voltage," SciencePG, doi: 10.11648/j.jjepe.20140303.13, May,30 2014.
- [2] Bruno Josso, Leif Larsen "Laplace transform numerical inversion", Kappa, June 2012.
- [3] Alan V. Oppenheim, George C. Verghese, "Signals, Systems, and Inference", Massachusetts Institute of Technology, 2010.
- [4] Patrick O. Kano, "Numerical Laplace Transform Inversion and Selected Applications", Applied Energetics, March 5, 2010.
- [5] Suraj Sharma S., Amir Ahmed, and Prateik Raj C., "Stability Analysis of DC-DC Boost Converter for Solar Electric Application", International Journal of Computer Applications, Volume 85-No2, January 2014.
- [6] Waleed K. Ahmed, "Advantages and disadvantages of using MATLAB/ode45 for solving differential equations in Engineering applications", UAE University, Abu Dhabi, Al-Ain, 15551, UE.
- [7] Aliyu B. Kisabo, C. A. Oshoku, Adetoro M.A Lanre, Aliyu Funmilayo A., "Ordinary Differential Equations: MATLAB/Simulink® Solutions.", International Journal of Scientific & Engineering Research, Volume 3, Issue 8, August-2012 1, ISSN 2229-5518.
- [8] Hadi Malek, "Control of Grid-connected Photovoltaic Systems Using Fractional Order Operators.", Utah State University Logan, Utah 2014.
- [9] Alejandro Gomez Yepes, "Digital Resonant Current Controllers for Voltage Source Converters", University of Vigo, Spain, December 14, 2011.
- [10] Carlos Andrés Ramos-Paja, Daniel González, Andrés Julián Saavedra-Montes, "Accurate calculation of settling time in second order systems: a photovoltaic application", Universidad Nacional de Colombia, Colombia, March, 2013.
- [11] Kourosh Raean, "A Study of The Gibbs Phenomenon in Fourier Series and Wavelets", The University of New Mexico, August, 2008
- [12] Michael A. B. Deakin, "The development of the Laplace transform, 1737-1937", Archive for History of Exact Sciences 30. XII. 1981, Volume 25, Issue 4, pp 343-390